Cell Cycle 14:4, 656–667; February 15, 2015; © 2015 Taylor & Francis Group, LLC

Human Nek7-interactor RGS2 is required for mitotic spindle organization

Edmarcia Elisa de Souza[1,2], Heidi Hehnly[3,4], Arina Marina Perez[1], Gabriela Vaz Meirelles[1], Juliana Helena Costa Smetana[1], Stephen Doxsey[3], and Jörg Kobarg[2,5,6,*]

[1]Laboratório Nacional de Biociências-LNBio; Centro Nacional de Pesquisa em Energia e Materiais-CNPEM; Campinas, SP Brasil; [2]Programa de Pós-graduação em Biologia Funcional e Molecular; Instituto de Biologia; Universidade Estadual de Campinas; Campinas, SP Brasil; [3]University of Massachusetts Medical School; Program in Molecular Genetics and Microbiology; Worcester, Massachusetts, MA USA; [4]University of Washington; Department of Pharmacology; Seattle, WA USA; [5]Universidade Estadual de Campinas; Instituto de Biologia; Departamento de Bioquímica e Biologia Tecidual; Campinas, SP Brasil; [6]Universidade Estadual de Campinas; Faculdade de Ciências Farmaceûticas; Campinas, SP Brasil

Keywords: cell division, mitotic spindle, mitotic spindle orientation, Nek7, RGS2

Abbreviations: CREST, calcium-responsive transactivator; EB1, end-binding protein 1; GAP, GTPase-activating protein; MT, microtubule; Nek, NIMA-related kinase; PCM, centrosomal pericentriolar material; PD, pull-down; PPI, protein-protein interaction; RGS, regulators of G protein signaling; WB, Western blotting; shRNA, short-interfering RNA.

The mitotic spindle apparatus is composed of microtubule (MT) networks attached to kinetochores organized from 2 centrosomes (a.k.a. spindle poles). In addition to this central spindle apparatus, astral MTs assemble at the mitotic spindle pole and attach to the cell cortex to ensure appropriate spindle orientation. We propose that cell cycle-related kinase, Nek7, and its novel interacting protein RGS2, are involved in mitosis regulation and spindle formation. We found that RGS2 localizes to the mitotic spindle in a Nek7-dependent manner, and along with Nek7 contributes to spindle morphology and mitotic spindle pole integrity. RGS2-depletion leads to a mitotic-delay and severe defects in the chromosomes alignment and congression. Importantly, RGS2 or Nek7 depletion or even overexpression of wild-type or kinase-dead Nek7, reduced γ-tubulin from the mitotic spindle poles. In addition to causing a mitotic delay, RGS2 depletion induced mitotic spindle misorientation coinciding with astral MT-reduction. We propose that these phenotypes directly contribute to a failure in mitotic spindle alignment to the substratum. In conclusion, we suggest a molecular mechanism whereupon Nek7 and RGS2 may act cooperatively to ensure proper mitotic spindle organization.

Introduction

The central mitotic spindle is composed of MT networks that connect kinetochores to the mitotic spindle poles.[1,2,3,4] In addition to the central spindle, astral MTs connect to spindle MTs via the spindle pole[5] generating forces to segregate chromosomes to mother and daughter cells. These events contribute to accurate assembly, positioning, and orientation of the mitotic spindle.[6,7,8] Failure of these processes can lead to cell death or chromosome instability, aneuploidy, and diseases, including cancer.[9,10]

Human serine/threonine-protein kinase, Nek7, is a member of NIMA-related kinase (Nek) family[11,12,13,14] required for proper spindle formation and mitotic progression.[15,16,17,18] Nek7 kinase activity reaches its maximum during mitosis[19,20] where it localizes to the centrosome to ensure appropriate mitotic progression.[15,16,17] In this regard, Nek7 loss reduces centrosomal localized pericentriolar material (PCM; e.g., pericentrin and γ-tubulin) during G2/M phase, arrests the cells in metaphase and subsequently causes apoptosis.[21,16,17,12,22] Additional studies have suggested Nek7′s involvement in cytokinesis.[18,23] Taken together, these studies indicate Nek7 as a regulator of cell cycle progression. However, the identification and characterization of bona fide downstream Nek7 substrates that participate in cell division remain unclear.

We have previously shown that the regulator of G-protein signaling, RGS2, interacts with Nek7 in yeast 2 hybrid screens and localizes with Nek7 at the central spindle and spindle poles.[24] This has led to the hypothesis that RGS2, like Nek7, might be required for spindle organization and function.

Regulators of G protein signaling (RGS) are canonically known to reform the inactive heterotrimeric (αβγ) G protein at the plasma membrane, in part, by acting as GTPase-activating proteins (GAPs) for several classes of G protein α subunits.[25,26] RGS2, one of the first mammalian RGS proteins identified,[27] is a negative regulator of Gα i and q.[28] Although several works have identified specific classes of G protein α subunits and their regulators as critical components in asymmetric cell division,[29,30] to date, no cell division function for RGS2 has been described.

In this study, we addressed the hitherto unknown characterization of RGS2 in regulating mitosis and mitotic spindle organization. The interaction and phosphorylation, the RGS2 spindle localization Nek7-dependent, as well as the similarities of mitotic phenotypes induced by Nek7 and RGS2, support the

*Correspondence to: Jörg Kobarg; Email: jorgkoba@unicamp.br
Submitted: 09/18/2014; Revised: 11/25/2014; Accepted: 11/28/2014
http://dx.doi.org/10.4161/15384101.2014.994988

interpretation that RGS2 may act cooperatively with Nek7 to regulate the proper organization and function of the mitotic spindle.

Results

Nek7 binds to and phosphorylates RGS2

We have previously described the identification of canonical negative regulator of heterotrimeric G protein signaling, RGS2, as a Nek7 interactor through yeast 2-hybrid.[24] To validate RGS2 as a Nek7 binding partner, we immobilized purified 6xHis-Nek7FL on Ni-NTA agarose beads and incubated the beads with HEK293T extract. In the pull-down we identified endogenous RGS2 (**Fig. 1A**) suggesting that the 2 proteins are present in the same complex. Furthermore, to confirm whether RGS2 could also behave as a Nek7 substrate, 6xHis-Nek7FL was incubated with [γ-^{32}P]ATP in the presence or absence of purified RGS2-GST, NEK9-GST (a known Nek7 substrate[24]), or GST-control. The 6xHis-Nek7FL was able to phosphorylate recombinant RGS2 and NEK9, but not GST-control (**Fig. 1B**), demonstrating that RGS2 was an *in vitro* Nek7 substrate. The band observed below the predicted recombinant 52 kDa RGS2 appears to be a degradation product (**Fig. 1B**).

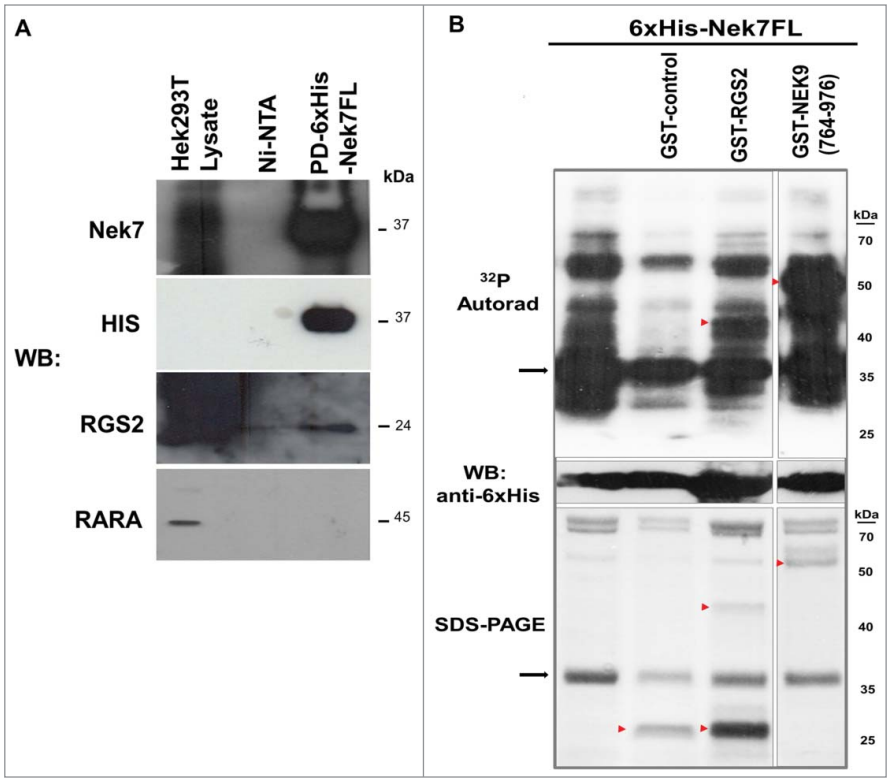

Figure 1. Interaction and, phosphorylation of Nek7 with RGS2. (**A**) Western Blotting (WB) analysis from pull-down (PD) of recombinant Nek7 binding to endogenous HEK293T RGS2. RGS2 does not bind to Ni-NTA agarose resins (Ni-NTA), nor does RARA bind to Nek7, demonstrating the assay specificity. The results are based on 3 independent experiments. Molecular weight (kDa) of the proteins is indicated. (**B**) Nek7 phosphorylates RGS2 *in vitro*. The arrowheads indicate the positions of the GST-tagged proteins or GST-control whereas the arrows indicate the position of the 6xHis-Nek7FL detected in the autoradiography (^{32}P Autorad), WB or in SDS-PAGE. The GST-NEK9(764–976) was used as a phosphorylation positive control.[24] No activity of 6xHis-Nek7FL was detected on GST-control, demonstrating the phosphorylation specificity for substrate. The results are based in 3 independent experiments. Molecular weights (kDa) of the marker proteins are indicated.

The RGS2 localization to the mitotic spindle is Nek7-dependent

To explore the functional involvement between Nek7 and RGS2, we investigated their *in vivo* cellular localization. We verified that endogenous RGS2 localized at the centrosome and to a subset of microtubules emanating from centrosome in a manner identical to α-tubulin during prometaphase (**Fig. 2A**). Furthermore, RGS2 localized at the spindle and to astral MTs during metaphase (**Fig. 2A**). Importantly, Nek7 localized along with RGS2 at the mitotic spindle and poles during prometaphase (**Fig. 2B**).These results raised the possibility that Nek7 and RGS2 might co-function in mitosis.

In order to further address this, we examined if Nek7 depletion affects RGS2 localization during mitosis (**Fig. 2C**). RGS2 localization to mitotic spindle and poles was severely reduced in Nek7-depleted cells (**Fig. 2D**), indicating that a precise level of Nek7 is critical to ensure proper recruitment of RGS2 to the mitotic spindle and poles. These findings are consistent with RGS2 being a novel Nek7 interactor and substrate and suggest that both work in concert to regulate mitotic progression. This is reinforced by the Protein-Protein Interaction (PPI) profile, visualized by a crosstalk network of Nek7 and RGS2 (**Fig. S1 and Table S1**).

RGS2 is involved in mitotic progression

Next, we examined the role of Nek7- (**Fig. 2C**) and RGS2-depletion (**Fig. 3A**) on mitotic progression. We noticed that both Nek7 (data not shown) and RGS2-depleted cells caused a similar increase in the mitotic index (5–6%) compared to control (2–3%) (**Fig. 3B**).

To determine at what point a mitotic delay occurred with either Nek7- or RGS2-depletion, live-cell imaging was performed. Compared to control, both Nek7- and RGS2-depleted cells had a significant increase in time spent between nuclear envelope breakdown to anaphase onset (~2-fold, **Fig. 3C**). Together, these findings indicate an involvement of Nek7 along with RGS2 in mitotic progression.

RGS2 depletion disrupts chromosomes segregation and mitotic spindle architecture

The mitotic delay following RGS2 depletion suggested a role for RGS2 in spindle formation. Based on this, we examined

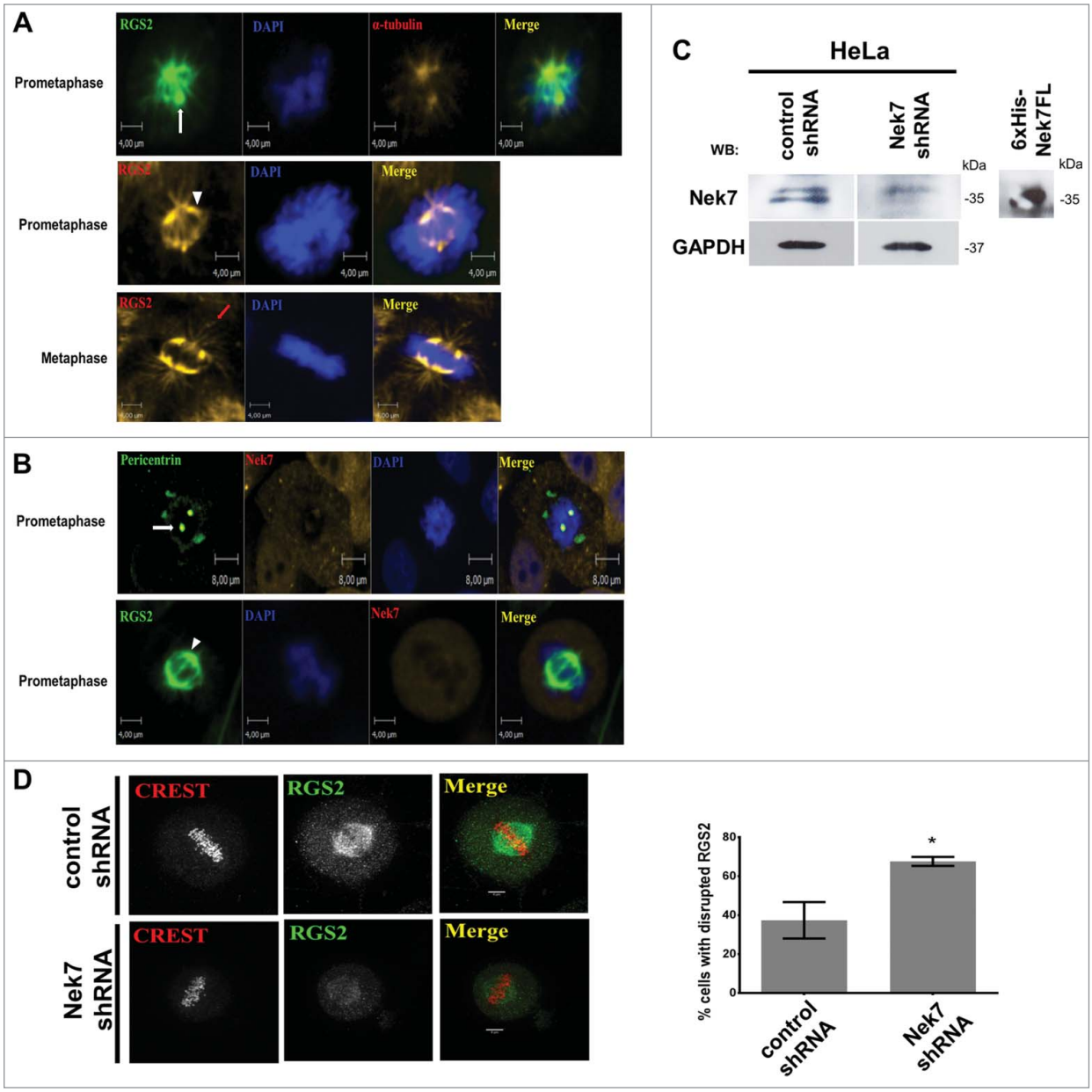

Figure 2. Nek7 suppression disrupts RGS2 recruitment to the spindle. (**A**) and (**B**) *In vivo* endogenous localization of RGS2 and Nek7 in HeLa cells during mitosis. Endogenous proteins were detected with specific primary antibodies, revealed with Alexa Fluor® 488 or Alexa Fluor® 546 secondary antibodies, and visualized by confocal fluorescence microscopy using Operetta High Content Imaging System (Perkin Elmer). The protein pericentrin was used to stain the centrosome and α-tubulin the cytoskeleton. The nucleus was stained by Hoechst. At least 20 cells were analyzed in each mitotic stage from 3 independent experiments and all cells showed the localization pattern represented in the images. The magnitude is indicated in the figures scale bars. White arrow denotes spindle pole (centrosome), arrowhead indicates mitotic spindle and red arrow indicates astral MTs. (**C**) Western Blotting (WB) analysis of lysates from HeLa cells treated with control shRNA or Nek7 shRNA, demonstrates the decreased levels of Nek7.WB of 6xHis-Nek7FL recombinant protein shows the antibodies specificity. GAPDH was used as a protein loading control. **(D)** Immunofluorescence images show loss of RGS2 at the spindle of Nek7-depleted cells. Bottom, graphs show the phenotype quantification. n = 35 counted cells/ triplicated experiments. *P < 0.05.

whether RGS2-depleted cells could appropriately align and assemble the MT-based mitotic spindle. Indeed, we found that RGS2-depleted metaphase cells exhibited misaligned kinetochores (CREST, **Fig. 4A-a′**). RGS2-depleted metaphase cells displayed DNA roughly aligned around a thicker metaphase plate (**Fig. 4B**), indicating defective congression of chromosomes to the metaphase plate. These misaligned chromosomes found in RGS2-depleted cells contained an elevated amount of Aurora B at their kinetochores (~3-fold- compared to control, **Fig. 4A-a′**), a hallmark of inappropriate kinetochore-MT attachment.[31,32]

One possibility for inadequate MT-kinetochore attachment is from a poorly functioning mitotic spindle and pole.[33] Strikingly, with RGS2 depletion, we found that MTs were poorly focused at mitotic spindle and poles during metaphase (EB1, **Fig. 4B** and

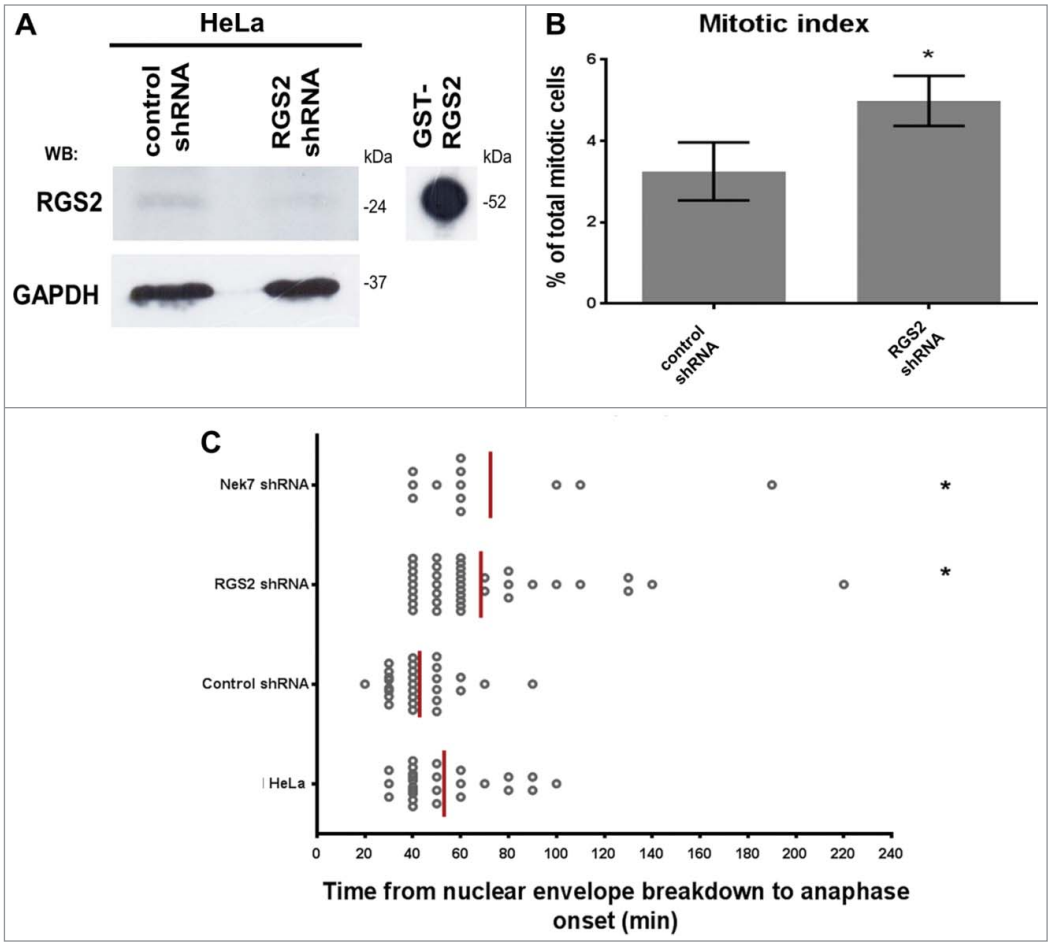

Figure 3. Nek7 and RGS2 depletion induces delay in mitosis. (**A**) Western Blotting (WB) analysis of lysates from HeLa cells treated with RGS2 shRNA or control shRNA demonstrates the decreased levels of RGS2. WB of GST-RGS2 recombinant protein shows the antibodies specificity. GAPDH was used as a protein loading control. (**B**) Statistical analysis of RGS2-depleted cells exhibiting higher mitotic index. Data represents means and standard deviations of 3 independent experiments. At least 750 cells were counted for each experimental group. (**C**) Timing in mitosis is extended in RGS2-depleted cells. Timing of individual cells (each spot) from nuclear envelope breakdown to anaphase onset (68,46 ± 5,791 min) compared with control shRNA (42,86 ± 2,763 min). Untreated HeLa cells (HeLa) are shown. Delay in mitosis is also observed in Nek7-depleted cells. Data represent means of 3 independent experiments.*$P < 0.05$. n = 60 in 3 independent experiments.

Aurora A, **Fig. 4C-c′**, respectively) and in some cases it resulted in a kinked spindle (Fig. 4B). Moreover, Aurora A is poorly concentrated at the mitotic spindle pole, which is required for bipolar spindle assembly (**Fig. 4C-c′** and for a review see refs. 34).

Since RGS2-depleted cells had unfocused MTs and chromosome misalignment, a problem with kinetochore fiber formation was suggested. Spindle MTs acetylation is closely correlated with kinetochore fiber MT stability.[35] Therefore, we examined acetylated MTs in RGS2-depleted metaphase cells. Acetylated-α-tubulin was severely reduced in RGS2-depleted cells compared to control (**Fig. 4D**).

Nek7 and RGS2 are important for integrity of spindle poles

Due to RGS2 spindle pole localization (**Figs. 2A and B**) and its depletion leading to unfocused MTs in metaphase cells (**Figs. 4B and C**), we examined whether MT-nucleation factors (e.g., pericentrin and γ-tubulin)[36,37,38] were recruited properly in RGS2-depleted cells.

Control metaphase cells have a robust focusing of γ-tubulin at the mitotic spindle pole with few dispersed γ-tubulin puncta (**Fig. 5A**). However, RGS2-depleted cells had a significant decrease in γ-tubulin at the mitotic spindle pole, with an increase in visible punctate staining throughout the cell (**Fig. 5A**). Consistent with previous reported effects of Nek7,[17,22] γ-tubulin was reduced in cells overexpressing FLAG-Nek7FL or dominant negative FLAG-Nek7KD (**Fig. 5B, columns 2 and 3**), concomitantly, there was a decrease in γ-tubulin at the mitotic spindle pole of Nek7 or RGS2-depleted cells (**Fig. 5B, column 4**). In addition to γ-tubulin, pericentrin fragmentation could also be observed in RGS2-depleted cells (**Fig. 5C**). Furthermore, we noted that the localization of p150Glued, a subunit of dynein/dynactin complex, that mediates MTs capture events at the cortex,[39] is dispersed at the spindle poles of RGS2-depleted cells (**Fig. 5D**). These results show that RGS2 contributes to mitotic spindle pole assembly and further corroborate the importance of Nek7 activity in the spindle pole functions.

RGS2 depletion affects spindle orientation

The mitotic delay and loss of spindle organization following RGS2-disruption indicated that RGS2 may have additional mitotic functions. Previous studies have argued that misorientation of the division plane causes a delay in flattening of the daughter cell farthest away from the substrate.[40,33] Closer inspection of our live-cell imaging experiments revealed that RGS2-depleted cells had a misorientation of their cell division axis (**Fig. 6A** and **Movie S3**) whereas control cells usually divide parallel to the substratum (**Fig. 6A** and **Movie S4**). Consistent with this, the spindle angle relative to the cell-substrate adhesion plane in ~35% of RGS2-depleted cells was >20°, where most control

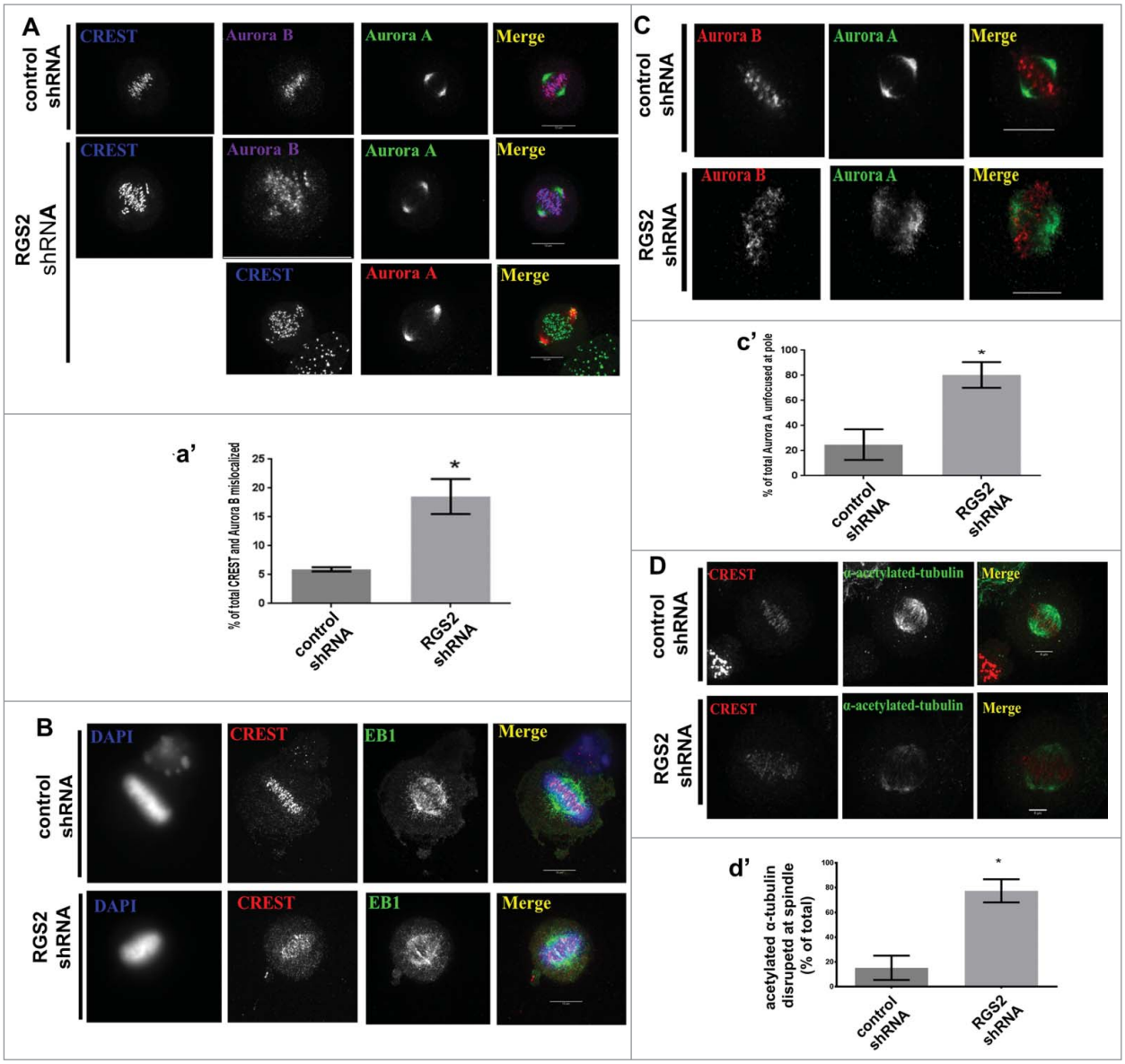

Figure 4. RGS2 loss affects the correct morphology of mitotic spindle and poles. (**A**) RGS2-depleted cells show misaligned chromosomes, unattached kinetochores (CREST and Aurora B staining), and (**B**) poorly focused spindles (CREST and EB1 staining). Graphs (**a**′) show the percentage of cells with CREST and Aurora B mislocalized. Thickened metaphase plate (DAPI) and elongated, kinked and curved spindle morphology (Aurora A staining) could also be observed. n>20/3 independent experiments. (**C**) Unfocused spindle poles in RGS2-depleted cells. Graphs (**c**′) show the percentage of cells with unfocused spindle poles. Scale bar in A and B is indicated in the images. Scale bar in C: 10 μM. (**D**) RGS2 depletion reduces MT-acetylation in mitotic spindle. Graphs (**c**′) show the percentage of cells with acetylated α-tubulin reduction at spindle. n>75/3 independent experiments. *$P < 0.05$.

spindles divided parallel to the substratum (90% < 20°, **Figs. 6B-C**). These results demonstrate that RGS2 is required for proper spindle orientation.

Since spindle positioning and orientation are controlled by pulling forces exerted on the plus-end of astral MTs interacting to cell cortex factors,[41] the precise distribution of astral and plus-end MTs to the cell cortex of control and RGS2-depleted cells were assessed. Interestingly, a severe loss of astral MTs was observed in RGS2-depleted cells by examining both α-tubulin and the plus-end binding protein EB1 (**Fig. 6D**), whereas control cells presented astral MTs that extend out to the cell cortex (**Fig. 6D**), suggesting that cortical interactions of MT astral were significantly impaired after RGS2 depletion.

Discussion

In this study we presented first evidence for RGS2 function in mitotic progression, spindle organization, and thus orientation. We propose that RGS2 has a role in mitosis is through its upstream kinase, has a Nek7.

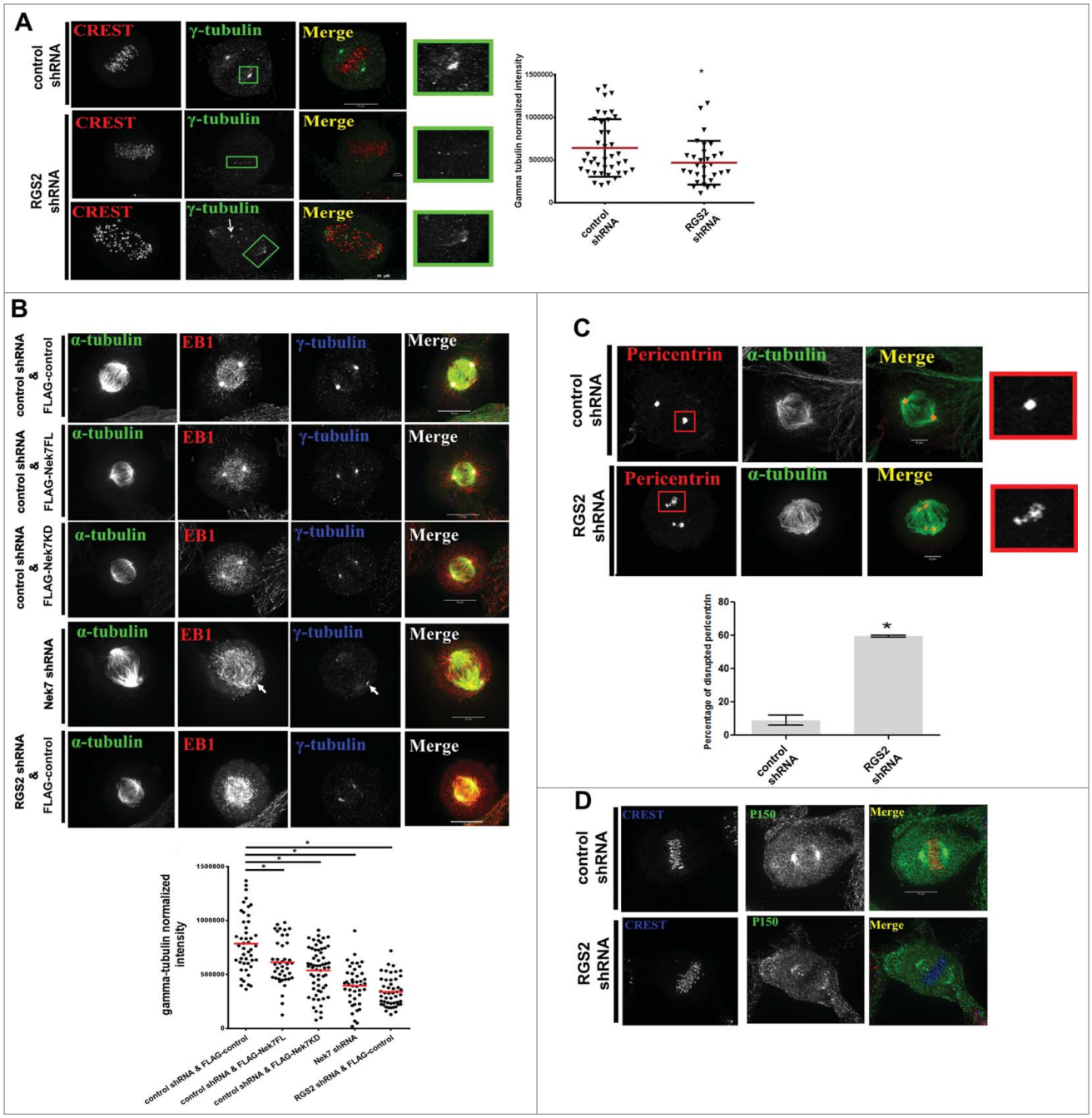

Figure 5. Nek7 and RGS2 suppression disrupt centrosomes integrity at the spindle poles. (**A**) Confocal images showing loss of poles γ-tubulin following RGS2 depletion. The arrow indicates punctate γ-tubulin staining. Bar graphs (right) showing the phenotype percentage are representative of 3 independent experiments. n > 30 cells for each experimental group. (**B**) Immunofluorescence images of mitotic cells showing loss of γ-tubulin from spindle poles (arrow) of cells presenting the indicated treatments. Graphs (bottom) show the phenotype percentage and are representative of 3 independent experiments. n = 25/ experimental group. (**C**) Confocal images showing the pericentrin disruption following RGS2 depletion. Bar graphs (bottom) showing the phenotype percentage. Data were obtained from 3 independent experiments. n> 20 cells for each experimental group. Insets on the right show higher magnification of centrosomal regions stained with γ-tubulin in (**A**) or pericentrin in **B**. *$P < 0.05$ by Student's t-test; error bars show standard deviations. (**D**) Immunofluorescence images of mitotic spindles show a p150Glued loss at the pole in RGS2-depleted cell compared to control.

Several findings in our study support this notion. First, we showed that Nek7 interacts with RGS2[24] and directly phosphorylates it *in vitro*. Second, Nek7 regulates the RGS2 mitotic spindle localization. Third, both Nek7 and RGS2 depletion led to a higher mitotic index accompanied by mitotic delay (**Figs. 3A and 3B**; for Nek7 see refs.[16,18]), with cells harboring chromosome alignment and kinetochore–microtubule attachment defects (**Figs. 4A and 4B**; for Nek7 see ref.[23]), disturbance in MT

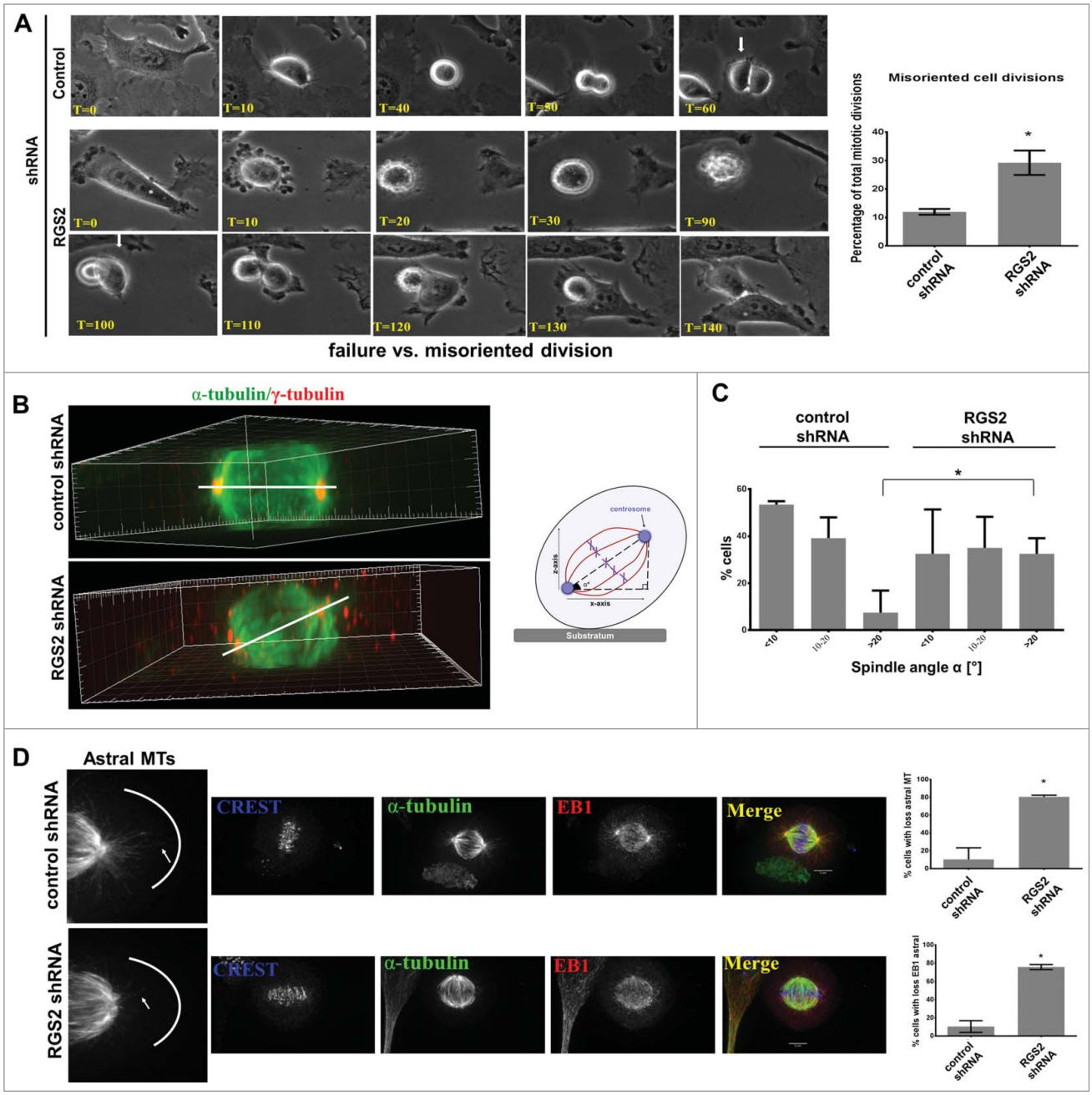

Figure 6. Loss of RGS2 causes spindle misorientation. (**A**) Frame series of time lapse live imaging movies show incorrect flattening of RGS2-depleted daughter cell onto the substrate after mitosis (misoriented cell division) (see text for details). Also uneven timing of division completion can be observed. Arrows indicate when the first daughter cell begins flatting. T = Time , min. Right: Graphs showing the increased percentage of misoriented cell division in RGS2-depleted cells. *P<0.05. (**B**) Side view of reconstructed 3-dimensional image shows RGS2-depleted cell exhibiting a high degree of spindle tilting relative to the cell-substratum adhesion plane compared to control cell. Spindle angle (α°) (bar) in RGS2 depleted-cell = 60°; α° in control cell = 0°. Right: Schematic of the angle of rotation in misoriented cell division. (**C**) The spindle angle is increased in RGS2-depleted cells. Graphs show RGS2-depleted cells with significant increase of spindle angle >20°. Spindle (α-tubulin), centrosomes (γ-tubulin) and/or PLK1 were used to identify spindle poles. Data represent means and standard deviations of a total of 75 mitotic cells in 3 independent experiments. n = 25 counted cells/experiment. *P < 0.05 (**D**). RGS2 depletion impairs the astral MTs recruitment to the cell cortex. Left enlargements show astral MTs at the cell cortex. Right, graphs show the phenotypes quantification. n = 40 counted cells/triplicated experiments. *P < 0.05.

dynamics (**Fig. 4D**; for Nek7 see ref.[42]), as well as spindle centrosome nucleation failure (**Fig. 5**; for Nek7 see ref.[17]). In addition, we showed that expressing the phosphorylation mutant Nek7KD caused disrupted recruitment of γ-tubulin into the mitotic centrosome, corroborating previous data that Nek7 function loss affects spindle pole functions.[17,22]

We provide evidences that failure in chromosome alignment in RGS2-depleted cells could be the consequence of defective

kinetochore-microtubule attachment, since we found kinetochores containing Aurora B, the key player in correction of kinetochore-microtubule attachment defects.[43] In this respect, disturbance of MT dynamics, as shown by spindle-MTs acetylation disruption, would create inappropriate MT-kinetochore attachments. Thus, the absence of RGS2 affects the control of chromosomes alignment and MT dynamics that results in a failure to pull the sister chromatids apart. According, it has previously been shown that RGS2 interacts directly with α-tubulin via a short polypeptide within its amino-terminus (amino acids 41–60) and contributes to the neuronal cell differentiation via regulation of microtubule dynamics.[44]

Finally, the most prominent phenotype of silencing RGS2 expression was the induction of misoriented cell division. In this regard, we showed that the effects of RGS2 depletion on the spindle orientation are likely through the disruption of astral MTs, a prerequisite for orientation of the spindle.[41] These findings appeared particularly notable because emerging evidences suggest a critical role of G α proteins in the control of asymmetric cell division via a regulatory role in the positioning of the mitotic spindle.[45,46] In this scenario, RGS2 may accelerate the conversion of Gαi-GTP to Gαi-GDP, which can reassociate with Gαγβ to reform the heterotrimer, that in turn, recruits important components as NuMA/LGN to provide the anchor sites for dynein at the cortex from where it is thought to generate pulling forces on the mitotic spindle.[7]

Correct alignment of the mitotic spindle during cell division is crucial to maintain tissue organization, by ensuring an accurate distribution of genetic material and a normal division plane.[10] It has been documented that mutations in multiple members of Neks, including Nek1 and Nek8, are associated to the formation of cystic kidneys[47,48] and tumors.[49] According to this, our findings suggest Nek7 and RGS2 as excellent candidates for contributing to tissue development. In addition, the cancer phenotypes induced by Nek7, including chromosomes missegregation and disruption of MT dynamics, make it an attractive target candidate for screening of new anti-cancer drugs, as previous show for other related targets.[50,51]

Although the finer mechanistic details of the regulatory link between Nek7 and RGS2 in spindle function remain to be deciphered, we propose that RGS2 may cooperate with Nek7 to regulate mitotic spindle organization (**Fig. 7**). Mutagenesis and mass spectrometry experiments should dissect the interaction and phosphorylation sites of RGS2 and Nek7 and determine whether Nek7 directly regulates RGS2 to control spindle assembly.

Materials and Methods

Plasmid constructions and proteins

The versions of Nek7 designed FL (full-length; amino acids 1–302) and KD (kinase dead; the Nek7 kinase activity was abolished by substituting the invariable catalytical lysine residues 63 and 64 by alanine - K63A/K64A) were cloned in-frame with the FLAG tag in a pCDNAFLAG vector (FLAG-Nek7FL and FLAG-Nek7KD constructs, respectively). Proteins 6xHis-Nek7FL, GST-RGS2, GST-NEK9(764–976) and GST were obtained according to de Souza et al.[24]

In Silico analysis

The retrieved DNA sequences from yeast 2-hybrid were processed, annotated and integrated in interaction networks using the Integrated Interactome System (IIS) platform, created by National Laboratory of Biosciences, Brazil.[52] The biological processes and cellular components were attributed from the Gene Ontology (GO; http://www.geneontology.org/) database. The interaction network was visualized using Cytoscape 2.8.3 software.[53]

Affinity pull-down (PD) analysis

Candidate Nek7-interactor RGS2 was previously obtained from yeast 2-hybrid screens conducted as described elsewhere in de Souza et al., 2014.[24] To validate RGS2 as Nek7 interacting proteins we performed pull-down assays. For this purpose, the baits 6xHis-Nek7FLor 6xHis-RARA were expressed and purified from *Escherichia coli* BL21 according to previously described by de Souza et al.[24] 6xHis-RARA was used as a control since RARA (Retinoic acid receptor α) is not described to interact with Nek7. Recombinant proteins were bound to Ni-NTA agarose resin at 4°C for 45 min. The resins were then washed 3 times for 5 min with wash buffer (50 mMTris-HCl pH 8.0, 1% NP40 and protease inhibitor cocktail) and incubated at 4°C overnight with HEK293T cellular lysates produced by homogenization in lysis buffer (50 mMTris-HCl pH 7.5, 150 mMNaCl, 1 mM EDTA, 0.5% Triton X-100 and protease inhibitor cocktail). The pulled-down samples were washed 3 times in wash buffer and bound proteins were loaded on SDS-PAGE and analyzed by Western blotting (WB).

In vitro protein phosphorylation

To test the ability of Nek7 to phosphorylate RGS2 *in vitro*, GST-RGS2 as potential substrate, GST-NEK9(764–976) as a positive control and GST as a negative control (GST-control)(de Souza et al., 2014),[24] were incubated with or without 6xHis-Nek7FL, plus 100 μM ATP and 185 kBq [γ-^{32}P]ATP (222 TBq/mmol; NEN) at 25°C during 1 h. The reaction was stopped by addition of electrophoresis buffer and 10 μL of each reaction was resolved by SDS-PAGE.^{32}P incorporation was detected by autoradiography.

Cell Culture, plasmid transfection and viral transduction

HeLa cells were cultured in DMEM (Sigma-Aldrich) supplemented with 10% fetal bovine serum (FBS, Gemini) and 1% penicillin/streptomycin (Invitrogen) at 37°C in a humidified atmosphere with 5% CO2. We used mainly HeLa cells, which have been widely used to investigate various aspects of cell division, including spindle orientation.[54,46,40]

Cells were plated on glass coverslips in 6-well or 12-well dishes following incubation at 37°C for 24 hours.

Plasmid constructs FLAG-Nek7FL, FLAG-Nek7KD or pCDNAFLAG vector as a control (FLAG-control) were

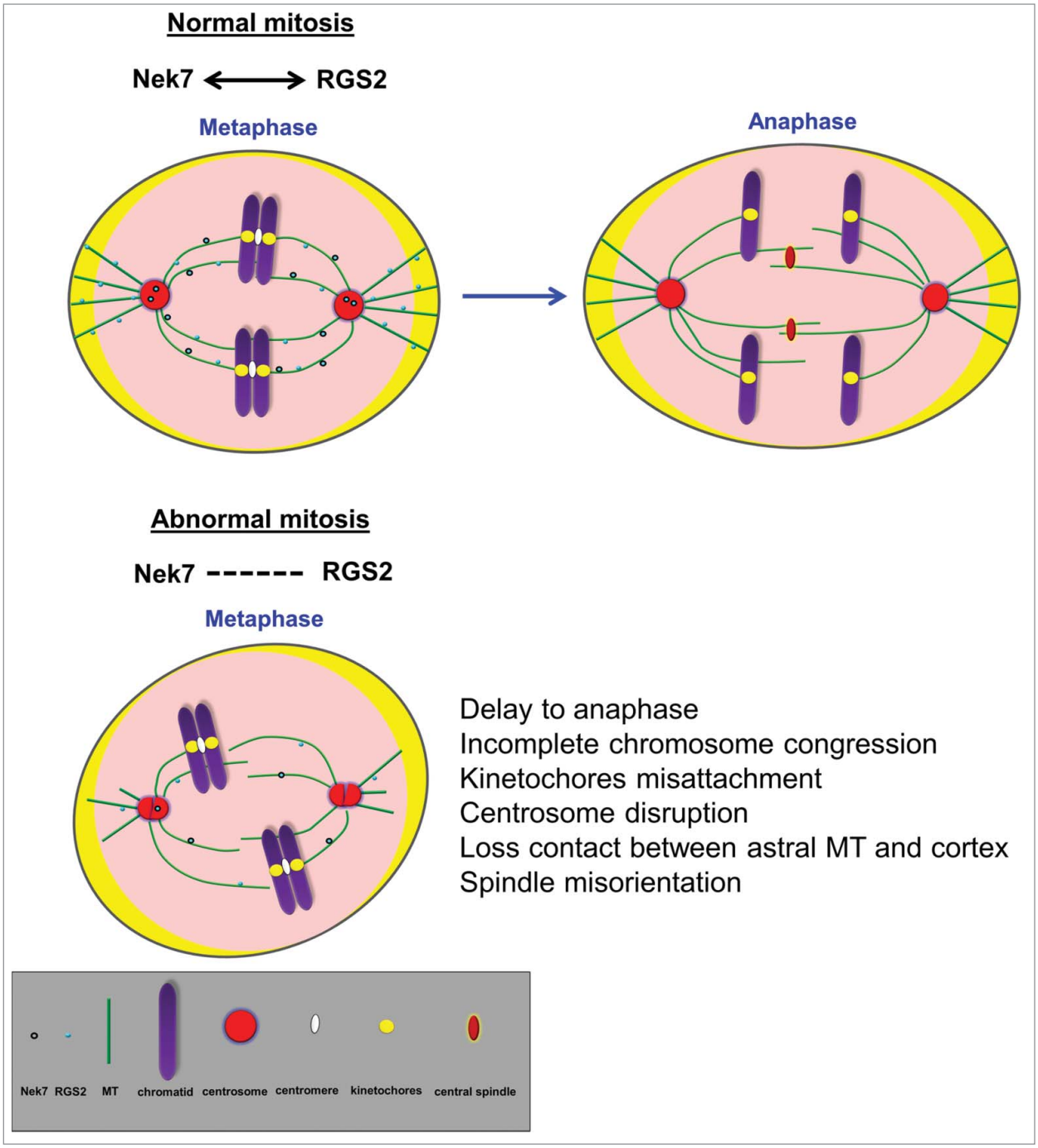

Figure 7. Nek7 and RGS2 act cooperatively to regulate mitotic spindle organization. Schematic representation of mitotic cell cycle. See detailed legend for symbols at the bottom of the figure.

transfected into HeLa cells using X-treme GENE DNA transfection reagent (Roche) according to the manufacturer's instructions.

Viral transduction was performed using lentiviral system carrying short-interfering RNAs (shRNAs) designed to target human Nek7 (Nek7 shRNA; 5′-CTTTAGTTGGTACGC CTTATT-3′), RGS2 (RGS2 shRNA; 5′-ACCCGTTTGAGC-TACTTCTTA-3) or GFP (control shRNA; 5′-GGCAAGCU-GACCCUGAAGUUC-3) purchased from The RNAi Consortium (TRC) (UMASSmed core, Worcester, USA). The shRNA targeting GFP was used as a control (shRNA control). The lentiviral particles were delivered to HeLa cells according to

manufacturers' instructions and stable HeLa cell lines were generated by selection with puromycin (Sigma-Aldrich) at 3.5 μg/ml. The depletion or overexpression efficacy of Nek7 and RGS2 was assessed by immunoblotting.

Antibodies

The primary antibodies used for immunofluorescence were: rabbit anti-RGS2 (abcam - ab36561, 1:200 dilution), goat anti-γ-tubulin (Santa Cruz - sc-7396, 1:200 dilution), human anti-CREST (Antibodies Inc. - 15–234, 1:200 dilution), mouse anti-aurora A (abcam - ab13824, 1:1000 dilution), rabbit anti-aurora B (abcam - ab2254, 1:1000 dilution), rabbit anti-EB1 (Sigma-Aldrich - E3406, 1:1000 dilution), rabbit anti-pericentrin (Stephen Doxsey Lab, 1:1000 dilution), mouse anti-pericentrin (Abcam -ab28144, 1:1000 dilution), mouse anti-α-tubulin FITC conjugate (abcam - ab64503, 1:300 dilution), mouse anti-acetylated α- tubulin (Sigma-Aldrich -Aldrich - T6793, 1:1000 dilution), mouse p150glued (BD Transduction - P50520–050, 1:200 dilution), rabbit anti-PLK1 (Cell signaling Technology - 4513P, 1:100 dilution). The mouse anti-His_5 (QIAGEN - 34660, 1:1000 dilution), mouse anti-GST (made *in house*), mouse anti-FLAG (Sigma-Aldrich - F1804, 1:1000 dilution), anti-Retinoic Acid Receptor α antibody (abcam - ab28767, 1:1000) antibodies were used for WB. Secondary antibodies for immunofluorescence staining for were obtained from the following sources: donkey anti-mouse AlexaFluor-488, donkey anti-goat AlexaFluor-488, donkey anti-rabbit AlexaFluor-488, chicken anti-rabbit Alexa Fluor-488, chicken anti-mouse Alexa Fluor-488, donkey anti-mouse Alexa Fluor-546, donkey anti-rabbit Alexa Fluor-546, donkey anti-mouse Alexa Fluor-549, donkey anti-goat Alexa Fluor-549, donkey anti-rabbit Alexa Fluor-549, donkey anti-goat Alexa Fluor-649, donkey anti-mouse Alexa Fluor-649, donkey anti-human AlexaFluor-649 (all from Invitrogen); horseradish peroxidase (HRP)-conjugated anti-mouse (Calbiochem) and HRP-linked antigoat or anti-rabbit secondary (Sigma-Aldrich) antibodies were used for WB purposes.

Immunofluorescence, microscopy and imaging software

Cells cultured on Cell Carrier plate (Perkin Elmer) were fixed and permeabilized with 3.7% formaldehyde solution (Sigma-Aldrich,F1635) containing 0.2% Triton X-100 in PBS 1X supplemented with 50 mM EGTA and 30 μg/mL taxol. Cells cultured on microscope coverslips (25 mm diameter) were washed with PBS (Sigma-Aldrich) and then fixed with methanol for 20 min. The fixation reagent was gently replaced by 1x PBS and the cells were then permeabilized and blocked for 30 min in blocking buffer containing 2% bovine serum albumin, 2% calf serum and 0.1% Triton X-100 (Sigma-Aldrich) into PBS. The cells were incubated for 1 h with primary antibodies diluted in blocking buffer. Cover slips or 384 Cell Carrier plate were gently washed with 1x PBS and incubated with respective secondary antibodies. DAPI was used to counterstain the nucleus. The cells from 384 Cell Carrier plate were observed by fluorescence microscopy using Operetta High Content Imaging System (PerkinElmer) and the images edited using Volocity Demo 6.1.1 software.

From the coverslips of HeLa, a series of Z stack images of mitotic cells were captured from 0.2 μm thick sections using a Perkin Elmer Ultraview spinning disk confocal microscope: Zeiss Axiovert 200, 100x Plan-APOCROMAT NA1.4 Oil, DIC lens and Hamamatsu ORCA-ER camera. The entire fixed cell volume was imaged and displayed as maximum projections using MetaMorph software (Molecular Devices) or processed for 3-D rendering using Imaris (Bitplane). Fluorescence range intensity was adjusted identically for each series of panels. Intensity profiles, linescan histograms and fluorescence intensity quantification were obtained from sum projections of Z stacks. Concentric circles pixels in diameter generated by MetaMorph were used to measure the fluorescence intensity of spindle poles (inner area) and local background (calculated as the difference between the outer and inner area).[40] MetaMorph software was used to visualize spindle orientation and to measure distances required to calculate spindle angle. Spindle angle measurements were performed from the linear (x–y plane) and vertical (z-axis) distance between spindle poles as previously described.[40]Graphs were created and analysis of statistical significance was performed by the Student t-test using GraphPad Prism software. Bars represent SE, $P < 0.05$ was considered as statistically significant.

Time Iapse image

Stable HeLa cell line was cultured in a chamber apparatus or glass-bottom 6-well tissue culture plates (MatTek) in complete medium with CO_2 exchange (0.5 Ls/ min) at 37°C. Cells were imaged every 10 min for 16 h using a 40× phase contrast lens. Images were captured on a Cool Snap HQ CCD camera (Roper Scientific) and concatenated using Metamorph software.

Disclosure of Potential Conflicts of Interest

No potential conflicts of interest were disclosed.

Acknowledgments

We thank Sambra Redick and John Schiel for technical assistance.

Funding

This work was financially supported by Fundação de Amparo à Pesquisa do Estado São Paulo (FAPESP, Grants #2010/51730–0 and # 2009–11912–5), Conselho Nacional de Pesquisa e Desenvolvimento (CNPq), and Centro Nacional de Pesquisa em Energia e Materiais (CNPEM). We also acknowledge the US National Institutes of Health contract NIH RO1 GM051994–14 and personal NIH grant to HH #NIH K99-GM107355.

Reference

1. Goshima G, Wollman R, Goodwin SS, Zhang N, Scholey JM, Vale RD, Stuurman N. Genes required for mitotic spindle assembly in Drosophila S2 cells. Science 2007; 5823:417-21; http://dx.doi.org/10.1126/science.1141314
2. Uehara R, Nozawa RS, Tomioka A, Petry S, Vale RD, Obuse C, Goshima G. The augmin complex plays a critical role in spindle microtubule generation for mitotic progression and cytokinesis in human cells.

Proc Natl Acad Sci USA 2009; 106:6998-7003; PMID:19369198; http://dx.doi.org/10.1073/pnas.0901587106
3. Dumont S, Mitchison TJ. Force and length in the mitotic spindle. Curr Biol 2009; 17:R749-61; http://dx.doi.org/10.1016/j.cub.2009.07.028
4. Hayward D, Metz J, Pellacani C, Wakefield JG. Synergy between multiple microtubule-generating pathways confers robustness to centrosome-driven mitotic spindle formation. Dev Cell 2014; 1:81-93; http://dx.doi.org/10.1016/j.devcel.2013.12.001
5. Luders J, Stearns T. Microtubule-organizing centres: a re-evaluation. Nat Rev Mol Cell Biol 2007; 8:161-167; PMID:17245416; http://dx.doi.org/10.1038/nrm2100
6. Willard FS, Kimple RJ, Siderovski DP. Return of the GDI: the GoLoco motif in cell division. Annu Rev Biochem 2004; 73:925-951; PMID:15189163; http://dx.doi.org/10.1146/annurev.biochem.73.011303.073756
7. Kotak S, Gönczy P. Mechanisms of spindle positioning: cortical force generators in the limelight. Curr Opin Cell Biol 2013; 6: 741-48; http://dx.doi.org/10.1016/j.ceb.2013.07.008
8. Zheng Z, Wan Q, Liu J, Zhu H, Chu X, Du Q. Evidence for dynein and astral microtubule-mediated cortical release and transport of Gαi/LGN/NuMA complex in mitotic cells. Mol Biol Cell 2013; 7:901-13; http://dx.doi.org/10.1091/mbc.E12-06-0458
9. Musacchio A, Salmon ED. The spindle-assembly checkpoint in space and time. Nat Rev Mol Cell Biol 2007; 8:379-93; PMID:17426725; http://dx.doi.org/10.1038/nrm2163
10. Noatynska A, Gotta M, Meraldi P. Mitotic spindle (DIS) orientation and DISease: cause or consequence? J Cell Biol 2012; 7:1025-35; http://dx.doi.org/10.1083/jcb.201209015
11. O'Connell MJ, Krien MJ, Hunter T. Never say never. The NIMA-related protein kinases in mitotic control. Trends Cell Biol 2003; 5:221-8; http://dx.doi.org/10.1016/S0962-8924(03)00056-4
12. O'Regan L, Blot J, Fry AM. Mitotic regulation by NIMA-related kinases. Cell Div 2007; 29:2-25.
13. Fry AM, O'Regan L, Sabir SR, Bayliss R. Cell cycle regulation by the NEK family of protein kinases. J Cell Sci 2012; 125:4423-4433; PMID:23132929; http://dx.doi.org/10.1242/jcs.111195
14. Meirelles GV, Perez AM, de Souza EE, Basei FL, Papa PF, Hanchuk TDM, Cardoso VB, Kobarg J. "Stop Ne (c)king around:" How systems biology can help to characterize the functions of NEK family kinases from cell cycle regulation to DNA damage response. World J Biol Chem 2014; 5(2):141-160.
15. Roig J, Groen A, Caldwell J, Avruch J. Active Nercc1 protein kinase concentrates at centrosomes early in mitosis and is necessary for proper spindle assembly. Mol Biol Cell 2005; 16:4827-40; PMID:16079175; http://dx.doi.org/10.1091/mbc.E05-04-0315
16. Yissachar N, Salem H, Tennenbaum T, Motro B. Nek7 kinase is enriched at the centrosome, and is required for proper spindle assembly and mitotic progression. FEBS Lett 2006; 27:6489-95; http://dx.doi.org/10.1016/j.febslet.2006.10.069
17. Kim S, Lee K and Rhee K. NEK7 is a centrosomal kinase critical for microtubule nucleation. Biochem Biophys Res Commun 2007; 1:56-62; http://dx.doi.org/10.1016/j.bbrc.2007.05.206
18. O'Regan L, Fry AM. The Nek6 and Nek7 protein kinases are required for robust mitotic spindle formation and cytokinesis. Mol Cell Biol 2009; 14:3975-90; http://dx.doi.org/10.1128/MCB.01867-08
19. Belham C, Roig, J, Caldwell JA, Aoyama Y, Kemp BE, Comb M, Avruch JA. mitotic cascade of NIMA family kinases. Nercc1/NEK9 activates the NEK6 and NEK7 kinases. J Biol Chem 2003; 37: 34897-909; http://dx.doi.org/10.1074/jbc.M303663200
20. Richards MW, O'Regan L, Mas-Droux C, Blot JM, Cheung J, Hoelder S, Fry AM, Bayliss R. An autoinhibitory tyrosine motif in the cell-cycle-regulated NEK7 kinase is released through binding of NEK9. Mol Cell. 2009; 4:560-70; http://dx.doi.org/10.1016/j.molcel.2009.09.038
21. Quarmby LM, Mahjoub MR. Caught Nek-ing: cilia and centrioles. J Cell Sci 2005; 118:5161-69; PMID:16280549; http://dx.doi.org/10.1242/jcs.02681
22. Kim S, Rhee K. NEK7 is essential for centriole duplication and centrosomal accumulation of pericentriolar material proteins in interphase cells. J Cell Sci 2011; 124:3760-70; PMID:22100915; http://dx.doi.org/10.1242/jcs.078089
23. Salem H, Rachmin I, Yissachar N, Cohen S, Amiel A, Haffner R, Lavi L, Motro B. Nek7 kinase targeting leads to early mortality, cytokinesis disturbance and polyploidy. Oncogene 2010; 28:4046-57; http://dx.doi.org/10.1038/onc.2010.162
24. de Souza EE, Meirelles GV, Godoy BB, Perez AM, Smetana JH, Doxsey SJ, McComb ME, Costello CE, Whelan SA, Kobarg J. Characterization of the human NEK7 interactome suggests catalytic and regulatory properties distinct from those of NEK6. J Proteome Res 2014; 13(9):4074-90; PMID:25093993; http://dx.doi.org/10.1021/pr500437x
25. Abramow-Newerly M, Roy AA, Nunn C, Chidiac P. RGS proteins have a signalling complex: interactions between RGS proteins and GPCRs, effectors, and auxiliary proteins. Cell Signal 2006; 18:579-591; PMID:16226429; http://dx.doi.org/10.1016/j.cellsig.2005.08.010
26. Bastin G, Heximer SP. Rab family proteins regulate the endosomal trafficking and function of RGS4. J Biol Chem. 2013; 30:21836-49; http://dx.doi.org/10.1074/jbc.M113.466888
27. Siderovski DP, Hessel A, Chung S, Mak TW, Tyers M. A new family of regulators of G-protein-coupled receptors? Curr Biol 1996; 2:211-2; http://dx.doi.org/10.1016/S0960-9822(02)00454-2
28. Keys JR, Greene EA, Koch WJ, Eckhart AD. Gq-coupled receptor agonists mediate cardiac hypertrophy via the vasculature. Hypertension 2002; 40:660-666; PMID:12411459; http://dx.doi.org/10.1161/01.HYP.0000035397.73223.CE
29. Wilkie TM, Kinch L. New roles for Gα and RGS proteins: communication continues despite pulling sisters apart. Curr Biol 2005; 15:843- 54; http://dx.doi.org/10.1016/j.cub.2005.10.008
30. Hewavitharana T, Wedegaertner PB. Non-canonical signaling and localizations of heterotrimeric G proteins. Cell Signal 2012; 1:25-34; http://dx.doi.org/10.1016/j.cellsig.2011.08.014
31. Lampson MA, Cheeseman IM. Sensing centromere tension: Aurora B and the regulation of kinetochore function. Trends Cell Biol 2011; 3:133-40; http://dx.doi.org/10.1016/j.tcb.2010.10.007
32. Hochegger H, Hégarat N, Pereira-Leal JB. Aurora at the pole and equator: overlapping functions of Aurora kinases in the mitotic spindle. Open Biol 2013; 3:120185; PMID:23516109; http://dx.doi.org/10.1098/rsob.120185
33. Hehnly H, Doxsey S. Rab11 endosomes contribute to mitotic spindle organization and orientation. Dev Cell 2014; 28:497-507; PMID:24561039; http://dx.doi.org/10.1016/j.devcel.2014.01.014
34. Cowley DO, Rivera-Pérez JA, Schliekelman M, He YJ, Oliver TG, Lu L, O'Quinn R, Salmon ED, Magnuson T, Van Dyke T. Aurora-A kinase is essential for bipolar spindle formation and early development. Mol Cell Biol 2009; 4:1059-71; http://dx.doi.org/10.1128/MCB.01062-08
35. Nagai T, Ikeda M, Chiba S, Kanno S, Mizuno K. Furry promotes acetylation of microtubules in the mitotic spindle by inhibition of SIRT2 tubulin deacetylase. J Cell Sci 2013; 19:4369-80; http://dx.doi.org/10.1242/jcs.127209
36. Zimmerman WC, Sillibourne J, Rosa J and Doxsey SJ. Mitosis-specific anchoring of gamma tubulin complexes by pericentrin controls spindle organization and mitotic entry. Mol Biol Cell 2004; 8:3642-57; http://dx.doi.org/10.1091/mbc.E03-11-0796
37. Bornens M. The centrosome in cells and organisms. Science 2012; 335:422-426; PMID:22282802; http://dx.doi.org/10.1126/science.1209037
38. Bouissou A, Vérollet C, de Forges H, Haren L, Bellaïche Y, Perez F, Merdes A, Raynaud-Messina B. γ-Tubulin ring complexes and EB1 play antagonistic roles in microtubule dynamics and spindle positioning. EMBO J 2014; 2:114-28; http://dx.doi.org/10.1002/embj.201385967
39. Laan L, Pavin N, Husson J, Romet-Lemonne G, van Duijn M, López MP, Vale RD, Jülicher F, Reck-Peterson SL, Dogterom M. Cortical dynein controls microtubule dynamics to generate pulling forces that position microtubule asters. Cell 2012; 3:502-14; http://dx.doi.org/10.1016/j.cell.2012.01.007
40. Delaval B, Bright A, Lawson ND, Doxsey S. The cilia protein IFT88 is required for spindle orientation in mitosis. Nat Cell Biol 2011; 4:461-8; http://dx.doi.org/10.1038/ncb2202
41. Lu MS, Johnston CA. Molecular pathways regulating mitotic spindle orientation in animal cells. Development 2013; 9:1843-56; http://dx.doi.org/10.1242/dev.087627
42. Cohen S, Aizer A, Shav-Tal Y, Yanai A, Motro B. Nek7 kinase accelerates microtubule dynamic instability. Biochim Biophys Acta 2013; 1833:1104-13; PMID:23313050; http://dx.doi.org/10.1016/j.bbamcr.2012.12.021
43. Welburn JP, Vleugel M, Liu D, Yates JR , Lampson MA, Fukagawa T, Cheeseman IM. Aurora B phosphorylates spatially distinct targets to differentially regulate the kinetochore-microtubule interface. Mol Cell 2010; 38(3):383-92; PMID:20471944; http://dx.doi.org/10.1016/j.molcel.2010.02.034
44. Heo K, Ha SH, Chae YC, Lee S, Oh YS, Kim YH, Kim SH, Kim JH, Mizoguchi A, Itoh TJ, Kwon HM, Ryu SH. Suh PG RGS2 promotes formation of neurites by stimulating microtubule polymerization. Cell Signal 2006; 12:2182-92; http://dx.doi.org/10.1016/j.cellsig.2006.05.006
45. Blumer JB, Kuriyama R, Gettys TW, Lanier SM. The G-protein regulatory (GPR) motif-containing Leu-Gly-Asn-enriched protein (LGN) and Gialpha3 influence cortical positioning of the mitotic spindle poles at metaphase in symmetrically dividing mammalian cells. Eur J Cell Biol 2006; 12:1233-40; http://dx.doi.org/10.1016/j.ejcb.2006.08.002
46. Woodard, Geoffrey E, Ning-Na Huang, Hyeseon Cho, Toru Miki, Gregory G Tall, and John H Kehrl. Ric-8A and Gi Alpha recruit LGN, NuMA, and dynein to the cell cortex to help orient the mitotic spindle. Mol Cell Biol 2010; 14: 3519-30; http://dx.doi.org/10.1128/MCB.00394-10
47. Upadhya P, Birkenmeier EH, Birkenmeier CS, Barker JE. Mutations in a NIMA-related kinase gene, Nek1, cause peliotropic effects including a progressive polycystic kidney disease in mice. Proc Natl Acad Sci U S A 2000; 97:217-221; PMID:10618398; http://dx.doi.org/10.1073/pnas.97.1.217
48. Zalli D, Bayliss R, Fry AM. The Nek8 protein kinase, mutated in the human cystic kidney disease nephronophthisis, is both activated and degraded during ciliogenesis. Hum Mol Genet 2012; 5:1155-71; http://dx.doi.org/10.1093/hmg/ddr544
49. Moniz L, Dutt P, Haider N, Stambolic V. Nek family of kinases in cell cycle, checkpoint control and cancer. Cell Div 2011; 1:18; http://dx.doi.org/10.1186/1747-1028-6-18
50. Kawamura E, Fielding AB, Kannan N, Balgi A, Eaves CJ, Roberge M, Dedhar S. Identification of novel small molecule inhibitors of centrosome clustering in cancer cells. Oncotarget 2013; 4: 1763-76; PMID:24091544
51. Sanhaji M, Ritter A, Belsham HR, Friel CT, Roth S, Louwen F, Yuan J. Polo-like kinase 1 regulates the stability of the mitotic centromere-associated kinesin in mitosis. Oncotarget 2014; 5: 3130-44; PMID:24931513

52. Carazzolle MF, de Carvalho LM, Slepicka HH, Vidal RO, Pereira GA, Kobarg J, Meirelles GV. IIS - Integrated Interactome System: a web-based platform for the annotation, analysis and visualization of protein-metabolite-gene-drug interactions by integrating a variety of data sources and tools. PLoS One 2014; 9(6):e100385; http://dx.doi.org/10.1371/journal.pone.0100385

53. Shannon P, Markiel A, Ozier O, Baliga NS, Wang JT, Ramage D, Amin N, Schwikowski B, Ideker T. Cytoscape: a software environment for integrated models of biomolecular interaction networks. Genome Res 2003; 11:2498-2504; http://dx.doi.org/10.1101/gr.1239303

54. Thoma CR, Toso A, Gutbrodt KL, Reggi SP, Frew IJ, Schraml P, Hergovich A, Moch H, Meraldi P, Krek W. VHL loss causes spindle misorientation and chromosome instability. Nat Cell Biol 2009; 8:994-1001; http://dx.doi.org/10.1038/ncb1912